Atmos. Chem. Phys. Discuss., 7, 11587–11619, 2007
www.atmos-chem-phys-discuss.net/7/11587/2007/

Atmospheric Chemistry and Physics Discussions

A compact and stable eddy covariance set-up for methane measurements using off-axis integrated cavity output spectroscopy

D. M. D. Hendriks, A. J. Dolman, M. K. van de Molen, and J. van Huissteden

Vrije Universiteit Amsterdam, Faculty of Earth and Life Sciences, Department of Hydrology and Geo-environmental Sciences, De Boelelaan 1085, 1081 HV Amsterdam, The Netherlands

Received: 12 July 2007 – Accepted: 30 July 2007 – Published: 6 August 2007

Correspondence to: D. M. D. Hendriks (dimmie.hendriks@falw.vu.nl)

Abstract

A DLT-100 Fast Methane Analyser (FMA) from Los Gatos Research (LGR) Ltd. is assessed for its applicability in a closed path eddy covariance field set-up. The FMA uses off-axis integrated cavity output spectroscopy (ICOS) combined with a highly specific narrow band laser for the detection of CH_4 and strongly reflective mirrors to obtain a laser path length of 2×10^3 to 20×10^3 m. Statistical testing, a calibration experiment and comparison with high tower data showed high precision and very good stability of the instrument. The measurement cell response time was tested to be 0.10 s. In the field set-up, the FMA is attached to a scroll pump and combined with a Gill Windmaster Pro 3 axis Ultrasonic Anemometer and a Licor 7500 open path infrared gas analyzer. The power-spectra and co-spectra of the instrument are satisfactory for 10 Hz sampling rates. The correspondence with CH_4 flux chamber measurements is good and the observed CH_4 emissions are comparable with (eddy covariance) CH_4 measurements in other peat areas.

CH_4 emissions are rather variable over time and show a diurnal pattern. The average CH_4 emission is 50 ± 12.5 nmol m^{-2} s^{-1}, while the typical maximum CH_4 emission is 120 ± 30 nmol m^{-2} s^{-1} (during daytime) and the typical minimum flux is -20 ± 2.5 nmol m^{-2} s^{-1} (uptake, during night time).

Additionally, the set-up was tested for three measurement techniques with slower measurement rates, which could be used in the future to make the scroll pump superfluous and save energy. Both disjunct eddy covariance as well as slow 1 Hz eddy covariance showed results very similar to normal 10 Hz eddy covariance. Relaxed eddy accumulation (REA) only matched with normal 10 Hz eddy covariance over an averaging period of at least several weeks.

ACPD

7, 11587–11619, 2007

1 Introduction

Methane is considered to be the third most important greenhouse gas globally, after water vapour and carbon dioxide. Its concentration has risen by 150% since the pre-industrial era (IPCC, 2007) and currently 20% of the enhanced greenhouse effect is due to methane (IPCC, 2007). Although methane is less abundant in the atmosphere compared to carbon dioxide, it is a relatively strong greenhouse gas: the Global Warming Potential (GWP) of methane is approximately 25 (over 100 years) while that of carbon dioxide is 1 (by definition; IPCC, 2007). Unfortunately, the low abundance of methane in the atmosphere hampers adequate concentration measurements of this gas. The eddy covariance technique, which requires both very precise concentration measurements and a high sampling rate, is therefore only sparsely applied for the assessment of methane emissions (Kroon et al., 2007; Hargreaves, 2001; Kormann, 2001). The advantages of the eddy covariance technique for measuring trace gases are none-the-less obvious: integrated continuous measurements over a larger footprint area and longer periods without disturbance from small scale surface features.

Since the eighties, infrared absorption spectrometry using tunable diode lasers (TDLs) has been widely used for measurements of trace gases in the lab. A field technique for eddy covariance using a multipass absorption cell was introduced in 1995 (Zahniser et al., 1995). Unfortunately, serious problems of drift and low sensitivity effects occurred. Additionally, the method had more practical drawbacks: the large nitrogen Dewar for temperature control that needs refill weekly, an extensive and sensitive optical module and frequent calibration. Improvements were made with the Quantum cascade laser (QCL) spectrometer which was first introduced in 1994 (Faist et al., 1994). The method proved to be more stable and accurate in eddy covariance set-up than the TDL spectrometry (Nelson et al., 2004; Kroon et al., 2007), but the practical drawbacks of the methane instruments (large nitrogen Dewar, optical module and frequent calibration) were still present in the QCL spectrometer technique. Hitherto, the micrometeorological measurement techniques for methane thus imply very

ACPD
7, 11587–11619, 2007

expensive, large and labour intensive field set-ups that are hard to maintain over a longer period and in remote areas.

We investigate here the applicability and quality of a Fast Methane Analyzer, a new off-axis ICOS technique using a highly specific narrowband laser and its applicability for eddy covariance field measurements of methane. The relatively user-friendly and low cost set-up is tested on precision and stability, the data processing is assessed and the first data series are analysed and compared with those obtained by existing techniques. Additionally, alternative measurements techniques of the set-up which reduce the power requirements are explored. Besides testing in the laboratory, experiments and measurements are performed at the Horstermeer measurement site, which is located in a eutrophic peat meadow area in the central part of the Netherlands and described extensively by Hendriks et al. (2007).

2 Measurement set-up and data processing

2.1 Experimental method and design

In 1998 a measurement cell with highly reflective mirrors was combined with a highly specific narrowband laser system (O'Keefe et al., 1998), creating a path length of at least two km in the measurement cell. In this way, small absorption rates cause much larger reduction of the total transmitted laser intensity. The ICOS technique could therefore be used for the detection of gases with ultra weak absorption, while making the extensive optical module and the nitrogen Dewar superfluous. The operation of the FMA is based on the ICOS technique and uses a distributed feedback (DFB) diode laser with a wavelength of nearly 1.65 μm. The DFB diode laser offers tunability, narrow line width and high output power in a compact and very rugged setup. It features a grating structure within the semi-conductor, which narrows the wavelength spectrum and guarantees single-frequency emission. Off-axis ICOS implies that he laser beam is directed into the measurement cell under a slight angle after which the laser beam is

reflected in the cell numerous times by highly reflective mirrors (reflectivity ~0.9999), thus creating a path length of 2×10^3 to 20×10^3 m (Bear et al., 2002; Fig. 1). The path length of the laser, and therefore the period over which the laser is being reflected in the measurement cell per measurement, might change as a result of changes in reflectivity of the mirrors in the measurement cell. This period over which the laser is being reflected in the measurement cell is called the mirror ringdown time (MRT) and is continuously monitored by the FMA. The final output signal of measured CH_4 concentration is determined from the reduction of laser intensity as a proportion of the MRT.

The FMA measures in the concentration range from 10 to 25×10^3 ppb and is claimed to have an accuracy of at least 1.0% and a precision of 0.1% and to operate autonomously. Technically, measurements can be made at rates up to 20 Hz and at ambient temperatures of 5 °C to 45 °C, while humidity should be below 95% to avoid condensation. In case of a measurement speed higher than 1 Hz, an external pump is needed to maintain the required response time. Internal voltage of the FMA should be maintained at 5.20 to 5.25 V and the pressure in the measurement cell should be between 190 and 210 hPa. The MRT may not drop below 3 to 3.5 μs, since the laser path length then becomes too short to detect the changes in laser intensity. The mirrors in the measurement cell are sensitive to dirt accumulating in the measurement cell; a small contamination of the measurement cell causes rapid decrease of the MRT. Cleaning the mirrors is a relatively simple procedure which can be done by the user himself in a dust-free environment. The measurement cell has a volume of 0.52×10^{-3} m^3 and a length of 0.21 m. Data output is provided in analogue as well as digital format (RS232&TCP/IP) and the device can store data up to 10 gigabytes. Warm-up time is approximately one minute and measurements as well as performance can be observed on a colour TFT LCD flat panel display. The dimensions of the FMA are 0.25 m height, 0.97 m width and 0.36 m depth and it has a weight of 22 kg. Power requirements are 115/230 VAC, 50/60 Hz and 180 W and inlet/outlet fittings are of the Swagelok type ($^3/_8$", $^1/_4$"). Also, a smaller rack mount version of the instrument exists which has the

ACPD
7, 11587–11619, 2007

same weight and price as well as the same power and fitting requirements, but has a smaller volume (0.22 m height, 0.61 m width and 0.48 m depth).

2.2 Design of closed path eddy covariance field set-up

The methane analyzer can be used in a closed-path eddy covariance field set-up (Fig. 2) with a scroll pump that creates the under pressure in the measurement cell which is required for the 10 Hz sampling rate. Here, a dry vacuum scroll pump (type XDS35i, BOC Edwards, Crawly, UK) is used with a maximum pumping speed of 1.0×10^{-3} m^3 s^{-1} requiring a 50 or 60 Hz energy supply with a voltage of 100/200 V to 120/230 V. The scroll pump is placed at the end of the set-up, connected to the FMA with a wire-reinforced tube with an internal diameter of 1.9×10^{-3} m, sucking air through the system. The FMA is placed in a heated, water resistant box, while the scroll pump is placed in an aerated box that prevents it from getting wet and from overheating. In addition to the internal Swagelok filter with a pore size of 2 μm, a filter with a pore size of 60 μm is placed at the inlet in order to prevent dust, aerosols, insects and droplets from entering the tubing. The inlet is shielded from the rain by a stainless steel cap. To prevent any water that accidentally passed the first filter from moving down towards the analyzer the air is first led up through a free steel tube (diameter of 6.4×10^{-3} m) that bends sharply at 0.5 m after which the air moves down towards the analyzer through a Teflon tube (diameter of 6.4×10^{-3} m). The high flow rate capacity of the scroll pump is dampened by the filters and tubings and creates an under pressure in the measurement cell of approximately 205 hPa. Using Boyle's law:

$$P_{\text{air}}\times V_{\text{air}}\approx P_{\text{cell}}\times V_{\text{cell}} \quad (1)$$

in which V is volume and P is pressure, it can be shown that the volume of the measurement cell of 0.52×10^{-3} m^3 contains only 0.11×10^{-3} m^3 of outside air (1010 hPa) under the prevailing pressure inside the measurement cell. After the air has passed trough the FMA measurement cell it flows trough the scroll pump and is exhausted trough a noise damper. The gas-inlet filter is positioned 0.2 m away from Licor 7500

ACPD
7, 11587–11619, 2007

open path infrared gas analyser (LI-COR Lincoln, NE, USA) and a Windmaster Pro 3 axis Ultrasonic Anemometer (GILL Instruments Limited, Hampshire, UK) directed to the main wind direction. Both instruments are installed at 4.3 m above the surface (Hendriks et al., 2007).

3 Performance of set-up and data treatment

3.1 Precision and instrument stability with 10 Hz sampling rate

The vertical flux (F_s) of an atmospheric property (s) can be directly determined by determining the covariance of that atmospheric property. This can be obtained by calculating the time averaged product of the deviation (s') of the atmospheric property (s), from $s=\overline{s}+s'$, and the deviation (w') of the vertical wind velocity (w) from $w=\overline{w}+w'$:

$$F_s=\overline{w's'}=\frac{1}{t_2-t_1}\int_{t_1}^{t_2} w'(t)s'(t)dt \quad (2)$$

(Aubinet et al., 2000). For this pur pose an instrument with high precision, system stability and high sampling rate in combination with short measurement cell response time is required. The applicability of the FMA for eddy covariance measurements was investigated by assessing these characteristics.

System stability is a major factor influencing high-sensitivity measurements. Theoretically, the signal from a perfectly stable system could be averaged infinitely. However, real systems are stable only for a limited time period. The length of time over which a laser signal can be averaged to achieve optimum sensitivity, and thus high precision, largely determines the quality of the spectrometer. Both maximum system stability and sensitivity can be determined using the Allan variance (Allan, 1966; Werle et al., 1993; Nelson et al., 2004; Kroon et al., 2007). The Allan variance (σ_A^2), as a function of integration time T, is the average of the sample variance of two adjacent averages of time

series of data and is described by Eq. (3):

$$\left\langle \sigma_A^2(k) \right\rangle_t = \frac{1}{2m} \sum_{s=1}^{m} [A_{s+1}(k) - A_s(k)]^2 \quad (3)$$

with: $A_s(k) = \frac{1}{k} \sum_{l=1}^{k} x_{(s+1)k+l}$, with: $s = 1, \ldots, m$ and $m = m' - 1$

In this equation A is an average, k is the number of elements in subgroup x, l is the first sample in a subgroup, s is the sub-sample number and m' the number of independent measurements. It is assumed that data are collected over a constant data interval Δt, therefore the integration time $T = k\Delta t$. Allan variance decreases when random noise dominates over drift effects. However, when noise caused by instrumental drift of the system starts to dominate, the Allan variance starts to increase, indicating a decrease of system stability and hence sensitivity. CH_4 concentration measurements over a ten minute period of relative constant CH_4 concentrations (Fig. 3) with a mean value of 1905 ppb and a standard deviation of 4.74 ppb with 10 Hz sampling rate were used to determine the Allan variance. Subsequently, the Allan variance of this period was plotted over the integration time T (Fig. 3), showing a decreasing Allan variance over integration times larger than 2.4 s. No increase of the Allan variance was observed at larger integration times, indicating an absence of instrumental drift, and thus high system stability and sensitivity, for integration times of a few seconds up to ten minutes. Additionally, an indication for the short term precision (σ) could be obtained by the y-axis interception point at the minimum Allan variance ($\sigma_{As}^2 = 6.1 \times 10^{-3}$ ppb^2). Using Eq. (4):

$$\sigma = \sigma_{As} \times f_s^{-1/2} \quad (4)$$

in which σ_{As} is the square root of the minimum Allan variance and f_s is the sampling frequency of the system (10 Hz), σ was determined as 7.81×10^{-3} ppb.

As long as ambient temperatures do not exceed the range of 5 to 45 °C, the DLT-100 the temperature (T_{cell}) will stay in a range tolerable for good performance. The pressure

ACPD
7, 11587–11619, 2007

in the measurement (P_{cell}) is mainly dependent on pump capacity, the amount and type of filtering and tubing, but should be kept in the range of 190 to 210 hPa. Within these boundary conditions the influence of changing temperature and pressure conditions in the measurement cel on CH_4 concentration measurements were assessed (Fig. 4). It can be observed that relatively large changes of T_{cell} as well as P_{cell} do not have an influence on the CH_4 concentration measurements. However, Tcell and Pcell do show a linear relation, in accordance with the ideal gas law.

A calibration experiment was carried out by administering standard gas mixtures with concentrations of 125 ppb and 2002 ppb CH_4 respectively, both with a precision of 0.2 ppb, to the FMA at ten moments within a 10-day period. During the whole experiment the FMA was never turned of in order to imitate longer measurement periods as will be the case in the field set-up. Although the measured concentration sometimes varied one or two ppb over the experimental period for both gases, no actual drift was observed in the analyser (Table 1). Calibration factors are 1 on average and fluctuate only very slightly.

Additionally, over a period of a week, CH_4 concentration measurements at the 4.3 m high tower at the Horstermeer site were compared with CH_4 concentrations measured at 20 and 60 m height at a measurement site in Cabauw (51°58′ N and 4°55′ E), approximately 30×10^3 m from the Horstermeer site [1]. The CH_4 concentrations at Cabauw were measured with a Carlo Erba gas Chromatograph system and have a precision of 2 ppb. The CH_4 concentration at the Horstermeer site was 15 ppb higher on average, which might be the result of the relatively high CH_4 emissions from the peat meadow area in which the measurements were taken. None the less, the increasing trend of CH_4 concentration at the Horstermeer site was similar to the trend at the Cabauw site. Generally, slow variation in concentrations is caused by the difference between continental and marine background concentration, the continental concentration being approximately 50 ppb higher (Eisma et al., 1994). During the measurement period,

[1] The CH_4 concentration measurements in Cabauw are measured with a gas chromatograph by the Energy Centre of the Netherlands (ECN).

ACPD
7, 11587–11619, 2007

winds from eastern, continental, direction prevailed, which accounted for the slow rise in CH_4 concentrations at the measurement locations.

In general a sampling rate of 10 Hz, with a Nyquist frequency of 5 Hz, is used for eddy covariance techniques (Aubinet et al., 2000; Kroon et al., 2007). The measurement rate of an instrument is determined by both electronic signal processing and by the signal response time of the measurement cell (τ) (Nelson et al., 2004). Electronic signal processing is dependent on the spectral complexity of the measurement technique as well as the technical design of the ICOS technique. In the case of the FMA, this was defined by the designers (LGR Ltd.) as 20 Hz. The limiting factor of the maximum sampling rate is often τ, which could be determined as the 63% ($1-^1/e$) of the instrument response after applying a step change in concentration at 20 Hz sampling rate (Moore, 1986; Zahniser et al, 1995). In this, sensitivity to tube length (Fig. 5) could be observed. Since the effect of tube damping is corrected separately, and τ only refers to the response of the instrument itself, the actual τ is determined as 0.10 s, which is in close agreement with the value expected from the volume of outside air in the measurement cell (0.11×10^{-3} m^3) divided by the pumping speed (1.0×10^{-3} m^3 s^{-1}). The τ includes an underestimation of 37% ($^1/e$) of the signal, which was corrected for during the data processing.

The time lag of the CH_4 measurements in the field set-up at a 10 Hz sampling rate was estimated at 0.6 s by determining the maximum covariance of w' and the deviation of the CH_4 concentration $[CH_4]'$ for w' at t=0.0 s and $[CH_4]'$ at t=0.1 s, t=0.2 s, t=0.3 s, etc.

3.2 Data treatment

Data were logged digitally on a handheld computer at a rate of 10 Hz (Van der Molen et al., 2006). The EUROFLUX methodology (Aubinet et al., 2000) was applied to the eddy covariance data to calculate the CO_2 fluxes from the open path system (Hendriks et al., 2007) and the CH_4 fluxes from the closed path system on a thirty minute basis. Since system instrumental drift was not observed, an overestimation of the fluxes as a

ACPD
7, 11587–11619, 2007

result of this averaging period was not expected. The effect of the measurement cell response time τ on the CH_4 signal was corrected for in the flux calculation procedure as well as for the time lag of 0.6 s between closed path CH4 and open path wind, temperature and CO_2 measurements. The tube length of the set-up was over 1000 times the length of the diameter of the tube and therefore the air temperature in the measurement cell can be considered stable. Therefore the Webb correction for density fluctuations arising from variations in temperature that was applied to the open path CO_2 measurements is not required for the closed path measurements of CH_4(Leuning and Moncrieff, 1990). The Webb correction for density fluctuations arising from variations in water vapour (measured with the Licor 7500) was applied according to Leuning and Moncrieff (1990). Frequency loss corrections for closed-path systems were applied according to the theory of Leuning and King (1992). The method of Nakai et al. (2006) was used to apply the angle of attack dependent calibration (Gash and Dolman, 2003; Van der Molen et al., 2004).

3.3 Validity of the measurement set-up and data

Spectral and co-spectral analysis of the fluctuations of w, air temperature (T) and CH_4 concentration [CH_4] in the atmosphere associated with turbulent transport are performed to assess the reliability of flux measurements (Stull et al., 1988; Kaimal and Finnigan, 1994). We determined spectra of the w, T and [CH_4] as well as co-spectra of temperature fluxes ($w'T'$) and CH_4 fluxes ($w'[CH_4]'$) using raw 10 Hz eddy covariance data of four 30 min periods in summer (Fig. 6). The power spectra and co-spectra are binned and plotted as a function of frequency on a log-log scale. Spectra for w, T and [CH_4] as well as the co-spectra $w'T'$ and $w'[CH_4]'$ have corresponding slopes showing a proportionality of $^{-2}/_{3}$, which is in agreement with the power law in the inertial sub-range (Eugster and Senn, 1994). This indicated that the eddy covariance set-up records nearly all fluctuations of [CH_4] associated with turbulent transport (Goulden et al., 1996) and that the measurements were taken in a well established surface layer. The performance of the eddy covariance set-up for CO_2 fluxes $w'[CO_2]'$ was

ACPD
7, 11587–11619, 2007

discussed in a previous paper by Hendriks et al. (2007). The shapes of the power- and co-variance spectra for [CH_4] were comparable to the [CO_2] spectra and the energy balance showed a closure of 82%. This implied that the data from the eddy covariance set-up are acceptable (Lloyd et al., 1996).

During night time periods with low friction velocity (u_*) the turbulence of the air can be too low for the performance of eddy covariance measurements. In order to determine the critical u_* values at this specific site (Wohlfahrt et al., 2005), the flux data for CH_4 and CO_2 of night time periods were plotted versus u_* (Fig. 7). The nightly CH_4 fluxes indeed decreased for u_*<0.09 m s^{-1} similar to the decrease in CO_2 flux.

4 CH_4 eddy covariance data-series and comparison with flux chamber measurements and high tower data

The CH_4 fluxes and CO_2 fluxes (net ecosystem exchange (NEE)) were plotted for a two week period in June 2006 at the Horstermeer site (Fig. 8). Both data series were corrected for low u_* values and gaps were filled with data of the surrounding half hours when small (max. two half hourly periods) or by data of the same point in time of the preceding day (max. ten half hourly periods). Although the CH_4 emissions are rather variable over time, a diurnal pattern can be observed with lower fluxes during the night and high fluxes during the day. CO_2 fluxes have a similar, but opposite, diurnal cycle. The average CH_4 emission was 50±12.5 nmol m^{-2} s^{-1}, while the typical maximum CH_4 emission was 120±30 nmol m^{-2} s^{-1} (during daytime) and the typical minimum flux was –20±2.5 nmol m^{-2} s^{-1} (uptake, during night time). Uncertainties of the CH_4 emissions were estimated at 25% of the half hourly flux data, based on uncertainty estimates of CO_2 eddy covariance data resulting from errors in measurement set-up, data processing and gap filling (Hendriks et al., 2007).

For two days during the CH_4 eddy covariance measurement period at the Horstermeer peat meadow site, flux chamber measurements were made in the footprint of the eddy covariance tower with a Photo Acoustic Field Gas-Monitor (type 1312, In-

nova AirTech Instruments, Ballerup, Denmark) connected with tubes to closed, dark chambers (Hendriks et al., 2007). Flux chamber data were collected at the three land elements occurring in the footprint of the eddy covariance tower: relatively dry peat land, saturated peat land and ditch water surfaces. The fluxes from the various land elements are averaged with respect to their relative surface area (70%, 20% and 10% respectively; Hendriks et al., 2007)). At the 10 June the flux chamber measurements showed an average CH_4 flux of 114±10 nmol m^{-2} s^{-1}, while the eddy covariance measurements showed an average CH_4 flux of 83±21 nmol m^{-2} s^{-1} over the same period (Fig. 9). On the 3 of October the average CH_4 flux from the chamber measurements was 54±11 nmol m^{-2} s^{-1}, while that of the eddy covariance was 61±15 nmol m^{-2} s^{-1}.

5 Alternative eddy covariance measurement types

In eddy covariance, the sampling rate determines the number of samples that are taken out of an infinitely large number of samples. The higher the sampling rate, the higher the statistical reliability, which results in higher accuracy of the observed means and covariances (Van der Molen, 2002). In order to obtain reliable estimates of fluxes, a sampling rate of at least 10 Hz is generally used for eddy covariance techniques. However, measurements performed at lower rates than 10 Hz generate results of certain reliability too. Disjunct eddy covariance, slow 1 Hz eddy covariance and REA are possible alternatives for the preferred 10 Hz eddy covariance. These measurement techniques could make the external pump of the FMA eddy covariance set-up superfluous and thus save over half of the energy required for the eddy covariance set-up. This might be inevitable to operate the set-up it in remote places where 220 V is not available.

Disjunct eddy covariance uses a subset of the whole 10 Hz time series (Fig. 10) to

ACPD
7, 11587–11619, 2007

determine the flux of an atmospheric property F_s according to Eq. (5):

$$F_s = < w's' > = \frac{1}{N} \times \sum_{i=1}^{N} w'_i s'_i \quad (5)$$

where N is the subset of the data (Rinne et al., 2000 and 2001). Here, the disjunct eddy covariance method was tested by sampling the first data point of every 10 data points from the 10 Hz data set, thereby creating a time interval of 0.9 s between the sampling moments, while the measurement cell response time remained 0.10 s. To build a field set-up for disjunct 1 Hz eddy covariance a "snap sampling" instrument would have to be mounted in front of the inlet of the system to obtain samples that are sampled with a frequency of 1 Hz, while maintaining the sampling duration as short as possible ("snap"). This method would give the FMA an analysis time of 1.0 s instead of 0.10 s.

With slow 1 Hz eddy covariance, F_s is determined in the same manner as 10 Hz eddy covariance (Eq. 2), but with dt=1.0 s instead of 0.10 s. The method was tested by averaging each 10 consecutive data points of CH_4 concentration as well as wind velocity for all variables of the 10 Hz data set (Fig. 10), thereby simulating a slower sampling rate (1 Hz) with a longer response time (1.0 s instead of 0.10 s).

REA is a conditional sampling method in which air samples are drawn to two separate reservoirs depending on the direction of w. The criterion of valve switching was based on values of the standard deviation of w (σ_w), which is measured by a sonic anemometer at 10 Hz. The valve is activated according to the threshold condition $|w_0| = 0.6\sigma_w$. In the case of $-w_0 \leq w \leq w_0$ (deadband values), neither "up" nor "down" samples were taken, but samples are discarded from the sampling system (Graus et al., 2006). Here, we simulated REA by dividing all eddy covariance data points of one half hour measurement period into three data matrixes based on the direction of the w (upward, downward and deadband values). Next, the measured concentrations are summed and the turbulent flux of the scalar s (F_s) was determined according to Eq. (6):

$$F_s \approx b \times \sigma_w \times \Delta s \quad (6)$$

(Businger and Oncley, 1990), where b is the correction for the deadband and Δs the difference between the concentrations in the accumulation reservoirs (Bowling et al., 1999). Pattey et al. (1993) determined the value of b to be 0.56, but after testing for the measurement set-up investigated here, a b-value of 0.70 showed results most similar to the normal 10 Hz eddy covariance measurements.

Data were compared with normal 10 Hz eddy covariance data as half hourly data series and as daily averages over a two-week period (Table 2 and Fig. 11). The disjunct eddy covariance method resulted in CH_4 emissions that were in fact very similar 10 Hz eddy correlation data, but showed small random deviations at a half hourly basis. On daily basis the disjunct eddy covariance showed a maximum underestimation of –5.4%, while on average the underestimation was only –1.4%. The slow 1 Hz eddy covariance method rather constantly underestimated the normal 10 Hz eddy covariance by –15.5% on average, both on the half hourly and the daily basis. This underestimation was the effect of averaging turbulent perturbations, enabling the set-up to measure CH_4 molecules transported by high frequent atmospheric turbulence (>1 Hz). However, in the Horstermeer polder no daily patterns were found in the underestimation of the emission, which could be explained by the characteristics of the measurement location: a flat, open and windy grass land site with a well mixed atmosphere. A single correction factor of 1.18 could be applied to the slow 1 Hz eddy covariance data, after which the normal 10 Hz eddy covariance data were very well matched by the slow 1 Hz eddy covariance data. The REA method resulted in half hourly data that showed considerable random deviations from the normal 10 Hz eddy correlation data, having a standard deviation twice as large as that of the normal eddy covariance (Table 2). Additionally, on a daily basis the trends observed by the normal 10 Hz eddy covariance were not matched very well. However, the average deviation from the normal 10 Hz eddy covariance over the two-week period is only 0.3%, implying the method might be well suitable for estimating CH_4 emission over periods of at least weeks.

ACPD
7, 11587–11619, 2007

6 Conclusions

The new fast methane analyser, which uses the new off-axis integrated cavity output spectroscopy technique, was found to perform satisfactory in field and lab tests. Compared to other techniques the absence of a large nitrogen Dewar for cooling that would need weekly refill, the compact, narrow band and stable laser, the relatively user friendliness and low costs are considerable advantages. However, care should be taken when placing the instrument with a scroll pump in the field. The instrument should be kept dry and in ambient temperatures between 5°C and 45°C, while the scroll pump should be kept dry and cool. Contamination of the measurement cell should be prevented, since the mirrors inside the measurement cell are sensitive and only a small contamination might cause a rapid decrease in reflectivity of the mirrors and performance of the instrument. Cleaning of the mirrors, however, is a relatively simple procedure that can be done by the user himself in a dust-free environment.

The analysis of the Allan Variance indicated a high precision and system stability of the FMA. Additionally, since instrumental drift was observed neither in the calibration experiment nor in the comparison with high tower data, it was concluded that frequent calibration of the FMA is indeed not necessary. The measurement cell response time was tested to be 0.10 s with a 37% underestimation of the measured signal, which was corrected for during the data processing. As long as ambient temperatures do not exceed the range of 5 to 45 °C and pressure in the measurement cell is near 205 hPa, the CH_4 measurements are not affected by changes in temperature and pressure in the measurement cell. Concluding, the instrument appeared very well suitable for eddy covariance measurements.

The FMA eddy covariance system performed well, as shown by the power- and co-spectra as well as by the closure of the energy balance. CH_4 and CO_2 fluxes appeared to respond similar to low u_* values and therefore a u_* correction was applied for CH_4 fluxes in the same manner as for CO_2 fluxes. CH_4 emissions are rather variable over time and show a diurnal pattern. The average CH_4 emission is $50 \pm 12.5\,\mathrm{nmol\,m^{-2}\,s^{-1}}$,

ACPD
7, 11587–11619, 2007

while the typical maximum CH_4 emission is 120±30 nmol m^{-2} s^{-1} (during daytime) and the typical minimum flux is 20±2.5 nmol m^{-2} s^{-1} (uptake, during night time). These CH_4 fluxes are in agreement with the QCL flux measurements at managed peat meadow site in the Netherlands (Reeuwijk), where emissions are 40±31 nmol m^{-2} s^{-1} on average (Kroon et al., 2007) and average annual CH_4 emission of 30 nmol m^{-2} s^{-1} from peat lands in Germany and the Netherlands (Drösler et al., 2007). From the comparison of the eddy covariance measurements with flux chamber measurements was observed that the fluxes from the two techniques lie in the same order of magnitude. However, considering the fact that the flux chamber measurements are point measurements at the soil surface while the eddy covariance has a footprint of hundreds of square meters, some degree of variation may be expected.

Additionally, the set-up was tested for three measurement techniques with slower measurement rates, which could be used in the future to make the scroll pump superfluous and save energy. Both disjunct eddy covariance as well as slow 1 Hz eddy covariance showed results very similar to 10 Hz eddy covariance. Relaxed eddy accumulation performed less well on half hourly and daily basis. However, over periods of at least several weeks, net emission showed only a slight deviation from the normal 10 Hz eddy covariance data. It was concluded that, when using a scroll pump is not possible for technical or practical reasons; both disjunct eddy covariance and slow 1 Hz eddy covariance are reliable substitutes for normal 10 Hz eddy covariance.

Acknowledgements. This research project is performed in the framework of the European research programme Carbo Europe (contract number GOCE-CT2003-505572) and the Dutch National Research Programme Climate Changes Spatial Planning (www.klimaatvooruimte.nl). Also, we would like to thank our technical co-operators R. Stoevelaar and R. Lootens.

References

Allan, D. W.: Statistics of Atomic Frequency Standards, Pr. Inst. Electr. Elect., 54(2), 221–230, 1966.

Aubinet, M., Grelle A., Ibrom, A., et al.: Estimates of the annual net carbon and water exchange of forests: The EUROFLUX methodology, Adv. Ecol. Res., 30, 30, 113–175, 2000.

Bear, D. S., Paul, J. B., Gupta, M., et al.: Sensitive absorption measurements in the near-infrared region using off-axis integrated-cavity-output spectroscopy, Appl. Phys. B, 75, 261–265, 2002.

Bowling, D. R., Delany, A. C., Turnipseed, A. A., et al.: Modification of the relaxed eddy accumulation technique to maximize measured scalar mixing ratio differences in updrafts and downdrafts, J. Geophys. Res.-Atmos., 104(D8), 9121–9133, 1999.

Businger, J. A. and Oncley, S. P.: Flux Measurement with Conditional Sampling, J. Atmos. Ocean. Tech., 7(2), 349–352, 1990.

Drösler, M., Freibauer, A., Christensen, T. R., et al.: Observations and status of peatland greenhouse gas emissions in Europe. In: Dolman, A. J., Valentini, R. and Freibauer, A.: Observing the continental scale greenhouse gas balance, Chapter 8, to be published in Springer Ecological series, 2007.

Eisma, R., Vermeulen, A. T., and Kieskamp, W. M.: Determination of European methane emissions, using concentration and isotope measurements, Environ. Monit. Assess., 31, 197–202, 1994.

Faist, J., Capasso, F., Sivco, D. L., et al.: Quantum Cascade Laser – Temperature-Dependence of the Performance-Characteristics and High T0 Operation, Appl. Phys. Lett., 65(23), 2901–2903, 1994.

Gash, J. H. C. and Dolman, A. J.: Sonic anemometer (co)sine response and flux measurement I. The potential for (co)sine error to affect sonic anemometer-based flux measurements, Agr. Forest Meteorol., 119(3–4), 195–207, 2003.

Goulden, M. L., Munger, J. W., Fan, S. M. et al.: Measurements of carbon sequestration by long-term eddy covariance: Methods and a critical evaluation of accuracy. Glob. Change Biol., 2(3), 169–182, 1996.

Graus, M., Hansel, A. Wisthaler, A., et al.: A relaxed-eddy-accumulation method for the measurement of isoprenoid canopy-fluxes using an online gas-chromatographic technique and PTR-MS simultaneously, Atmos. Environ., 40, S43–S54, 2006.

Hargreaves, K. J., Fowler, D., et al.: Annual methane emission from Finnish mires estimated from eddy covariance campaign measurements, Theor. Appl. Climatol., 70(1-4), 203–213, 2001.

Hendriks, D. M. D., van Huissteden, J., Dolman, A. J., van der Molen, M. K.: The full greenhouse

gas balance of an abandoned peat meadow, Biogeosciences, 4, 411–424, 2007, http://www.biogeosciences.net/4/411/2007/.
IPCC: IPCC Fourth Assessment Report, Climate Change 2007, Cambridge Univ. press., Cambridge, UK, 2007.
Kaimal, J. C. and Finnigan, J. J.: Atmospheric boundary layer flows, their structure and management, New York, Oxford University Press, 33–65, 208–280, 1994.
Kormann R., Muller, H., Werle, P.: Eddy flux measurements of methane over the fen "Murnauer Moos", 11 degrees 11 ' E, 47 degrees 39 ' N, using a fast tunable diode laser spectrometer, Atmos. Environ., 35(14), 2533–2544, 2001.
Kroon, P. S., Hensen, A., Zahniser, M. S., et al.: Suitability of quantum cascade laser spectrometry for CH_4 and N_2O eddy covariance measurements, Biogeosciences Discuss., 2, 1137–1165, 2007, http://www.biogeosciences-discuss.net/2/1137/2007/.
Leuning, R. and Moncrieff, J. : Eddy-Covariance CO_2 Flux Measurements Using Open-Path and Closed-Path Co2 Analyzers – Corrections for Analyzer Water-Vapour Sensitivity and Damping of Fluctuations in Air Sampling Tubes, Bound.-Lay. Meteorol., 53(1–2), 63–76, 1990.
Leuning, R. and King, K. M.: Comparison of eddy-covariance measurements of CO_2 fluxes by open-path and closed path CO_2 analysers. Bound.-Lay. Meteorol., 59 (3), 297–311, 1992.
Nakai, T., van der Molen, M. K., Gash, J. H. C., et al.: Correction of sonic anemometer angle of attack errors, Agr. Forest. Meteorol., 136(1-2), 19–30, 2006.
Nelson, D. D., McManus, B., Urbanski, S., et al.: High precision measurements of atmospheric nitrous oxide and methane using thermoelectrically cooled mid-infrared quantum cascade lasers and detectors, Spectrochim. Acta. A, 60(14), 3325–3335, 2004.
O'Keefe, A.: Integrated cavity output analysis of ultra-weak absorption, Chem. Phys. Lett., 293(5–6), 331–336, 1998.
Pattey, E., Desjardins, R. L., and Rochette, P.: Accuracy of the Relaxed Eddy-Accumulation Technique, Evaluated Using CO_2 Flux Measurements, Bound.-Lay. Meteorol., 66(4), 341–355, 1993.
Rinne, H. J. I., Delany, A. C., Greenberg, J. P., et al.: A true eddy accumulation system for trace gas fluxes using disjunct eddy sampling method, J. Geophys. Res.-Atmos., 105(D20), 24 791–24 798, 2000.
Rinne, H. J. I., Guenther, A. B., Warneke, C., et al.: Disjunct eddy covariance technique for

trace gas flux measurements, Geophys. Res. Lett., 28(16), 3139–3142, 2001.
Stull, R. B.: An Introduction to boundary layer meteorology, Dordrecht, Kluwer Academic Publishers, Atmospheric Sciences Library, Chapter 8, 1988.
Van der Molen, M. K.: Meteorological impacts of land use change in the Maritime tropics, Chapter 3, Data analysis, Thesis, Vrije Universiteit, 35–72, 2002.
Van der Molen, M. K., Gash, J. H. C., Elbers, J. A., et al.: Sonic anemometer (co)sine response and flux measurement – II. The effect of introducing an angle of attack dependent calibration, Agr. Forest Meteorol., 122(1-2), 95–109, 2004.
Van der Molen, M. K., Zeeman, M. J., Lebis, J., et al.: EClog: A handheld eddy covariance logging system, Comput. Electron. Agr., 51(1–2), 110–114, 2006.
Werle, P., Mucke, R., and Slemr, F.: The Limits of Signal Averaging in Atmospheric Trace-Gas Monitoring by Tunable Diode-Laser Absorption-Spectroscopy (Tdlas), Appl. Phys. B-Photo, 57(2), 131–139, 1993.
Wohlfahrt, G., Anfang, C., Bahn, M., et al.: Quantifying nighttime ecosystem respiration of a meadow using eddy covariance, chambers and modelling, Agr. Forest Meteorol., 128(3–4), 141–162, 2005.
Zahniser, M. S., Nelson, D. D., McManus, J. B., et al.: Measurement of Trace Gas Fluxes Using Tunable Diode-Laser Spectroscopy. Philosophical Transactions of the Royal Society of London, Series a-Mathematical Physical and Engineering Sciences, 351(1696), 371–381, 1995.

Table 1. Results of the 10-day calibration experiment with two standard gases of 125 and 2002 ppb respectively. Time elapsed since start of experiment; CH_4 concentrations measured by FMA, deviation from the actual concentration and calibrations factor are shown.

measurement (date and time)		time elapsed (days)	concentrations measured with FMA: low CH_4 gas (125 ppb) (ppb)	(deviation)	high CH_4 gas (2002 ppb) (ppb)	(deviation)	calibration factor
2/4/07	11:50:00	0	125	3.3%	2005	0.2%	0.998
3/4/07	09:00:00	0.882	127	3.3%	1999	–0.1%	1.003
3/4/07	15:30:00	1.153	125	–0.6%	1999	–0.1%	1.002
4/4/07	09:20:00	2.896	125	–0.6%	2000	0.0%	1.001
4/4/07	16:45:00	2.205	125	–0.6%	1999	–0.1%	1.002
5/4/07	09:30:00	2.903	125	–0.6%	1999	–0.1%	1.002
5/4/07	17:30:00	3.236	124	–1.4%	2001	0.0%	1.000
10/4/07	09:45:00	7.913	125	–0.6%	2004	0.1%	0.999
11/4/07	09:40:00	8.910	125	–0.6%	2002	0.0%	1.000
11/4/07	16:30:00	9.194	125	–0.6%	2002	0.0%	1.000
12/4/07	09:15:00	9.892	125	–0.6%	2004	0.1%	0.999

ACPD
7, 11587–11619, 2007

Table 2. Summary of results of disjunct eddy covariance, slow 1 Hz eddy covariance (with and without correction factor) and REA compared to normal 10 Hz eddy covariance. Half hourly data, average emissions, standard deviations and deviation from the normal 10 Hz eddy covariance are shown for all measurement techniques.

	two week average		half hourly data		daily averages	
	emission ($nmol\,m^{-2}\,s^{-1}$)	deviation from 10 Hz data	stand. dev. ($nmol\,m^{-2}\,s^{-1}$)	max. deviation	stand. dev. ($nmol\,m^{-2}\,s^{-1}$)	max. deviation
normal 10 Hz EC	50.90	0.0%	23.46	0%	9.53	0.0%
disjunct 1 Hz EC	49.40	–1.4%	24.60	60%	9.50	–5.4%
slow 1 Hz EC	42.48	–15.2%	20.44	50%	7.89	–18.8%
slow 1 Hz EC (corrected with factor 1.18)	50.13	0.1%	24.12	35%	9.31	–4.2%
REA (d=0.6 and b=0.75)	49.93	–0.3%	47.92	> 100%	13.15	41.9%

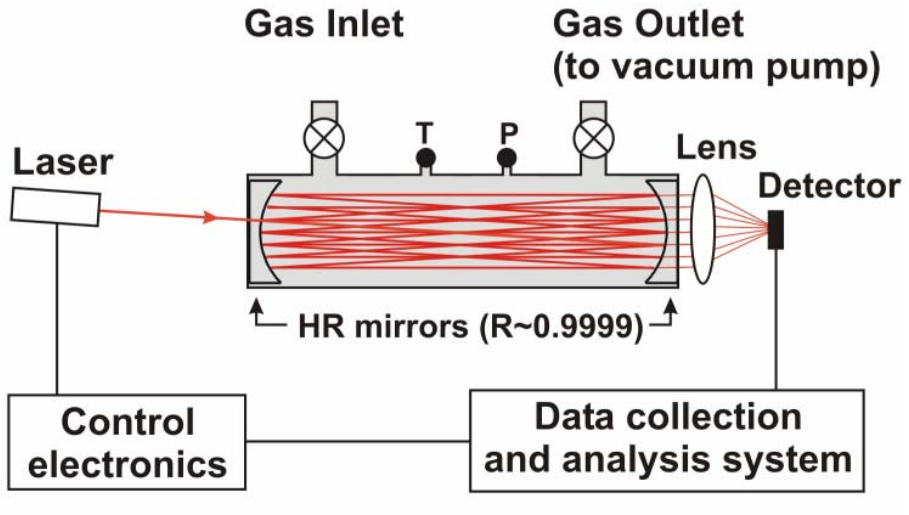

Fig. 1. Schematic overview of the off-axis integrated cavity output spectrometry (ICOS) technique used in the FMA. (Source: LGR Ltd.).

ACPD
7, 11587–11619, 2007

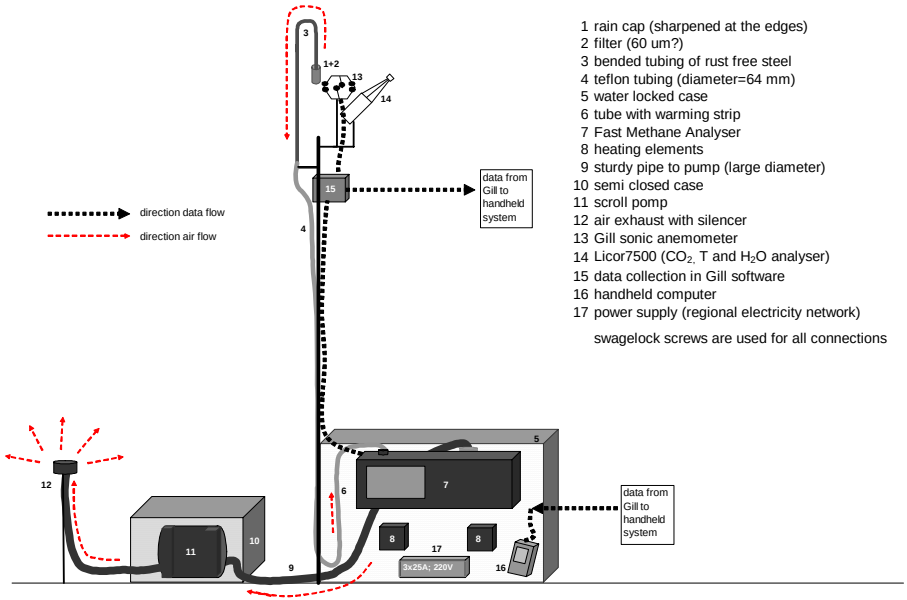

Fig. 2. Schematic overview of the combined field set-up of the open path eddy covariance system for carbon dioxide and water vapour and the closed path eddy covariance system for methane using the FMA.

ACPD
7, 11587–11619, 2007

EGU

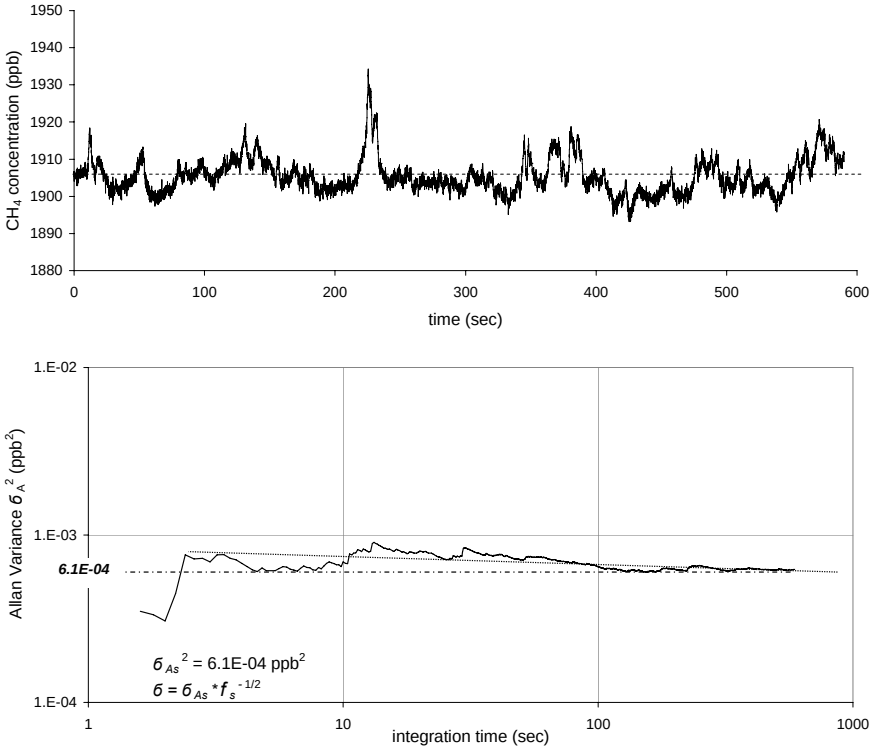

Fig. 3. Time series of CH_4 concentration measurements with 10 Hz sampling rate with a mean of 1905 ppb and a standard deviation of 4.74 ppb (upper graph) and the Allan variance plot over these data (lower graph).

ACPD
7, 11587–11619, 2007

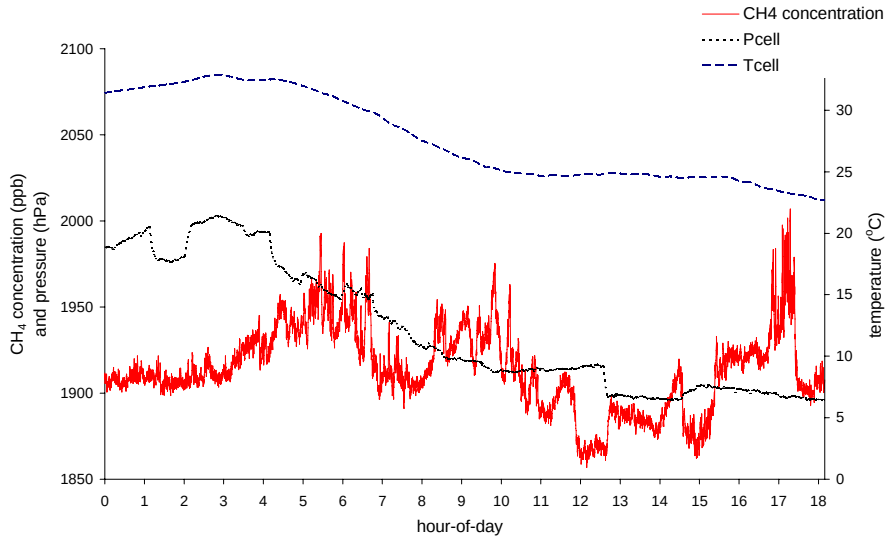

Fig. 4. FMA data from a measurement day in spring. P_{cell} ranges from 190 to 201 hPa and T_{cell} ranges from 22.7 to 32.9°C. Fluctuations in CH_4 concentration measurements show no dependence on P_{cell} or T_{cell}.

ACPD
7, 11587–11619, 2007

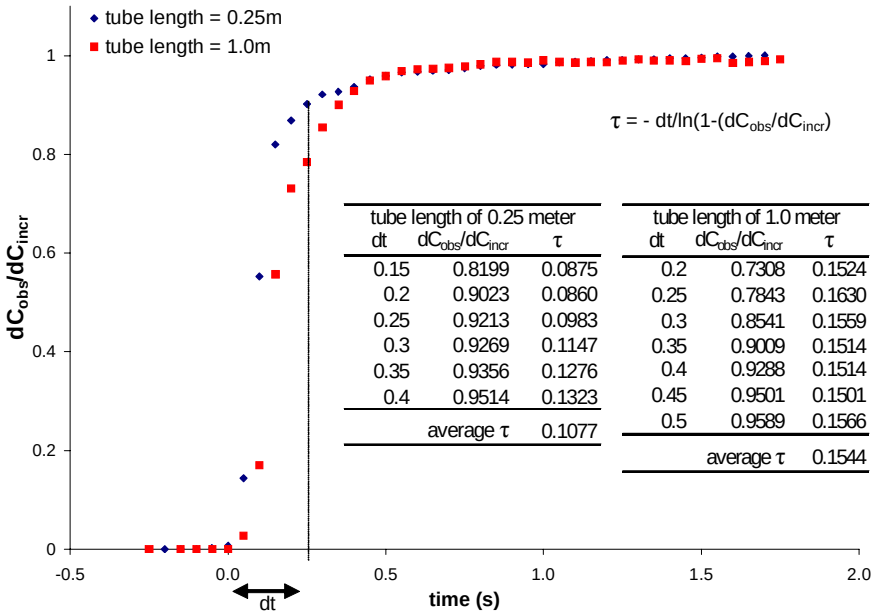

tube length of 0.25 meter		
dt	dC_{obs}/dC_{incr}	τ
0.15	0.8199	0.0875
0.2	0.9023	0.0860
0.25	0.9213	0.0983
0.3	0.9269	0.1147
0.35	0.9356	0.1276
0.4	0.9514	0.1323
	average τ	0.1077

tube length of 1.0 meter		
dt	dC_{obs}/dC_{incr}	τ
0.2	0.7308	0.1524
0.25	0.7843	0.1630
0.3	0.8541	0.1559
0.35	0.9009	0.1514
0.4	0.9288	0.1514
0.45	0.9501	0.1501
0.5	0.9589	0.1566
	average τ	0.1544

Fig. 5. Normalized and averaged time series showing 63% instrument response with 20 Hz sampling rate changing from ambient air to a gas sample with a high CH_4 concentration. Tables showing the values determined for t for tube lengths of 0.25 m and 1.0 m.

ACPD
7, 11587–11619, 2007

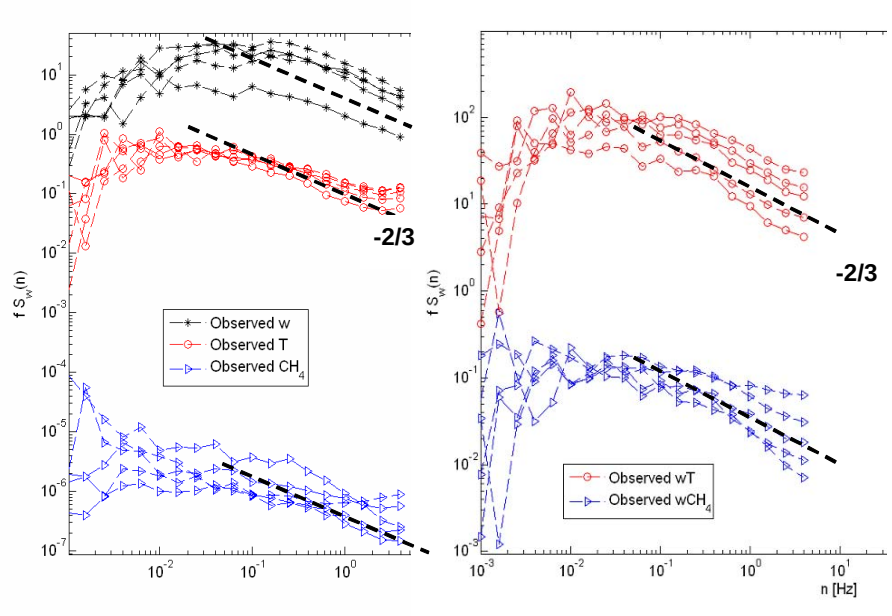

Fig. 6. Results from spectral analyses of w, T and [CH_4] and (co-)spectral analyses of $w'T'$ and $w'[CH_4]'$, showing the required slopes of $-^2/_3$ under turbulent circumstances. Analyses were done over four half hours of 10 Hz data which were separately binned.

ACPD
7, 11587–11619, 2007

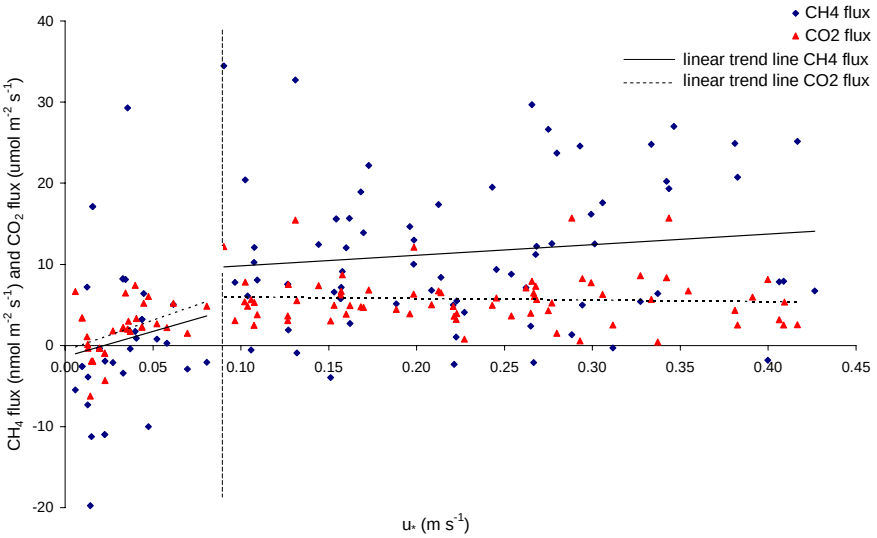

Fig. 7. Results of the analyses of the effect of variation in u_* on nightly CH_4 and CO_2 fluxes, showing a drop in flux magnitude below of u_* values of 0.09 m s^{-1} for both CH_4 and CO_2.

ACPD
7, 11587–11619, 2007

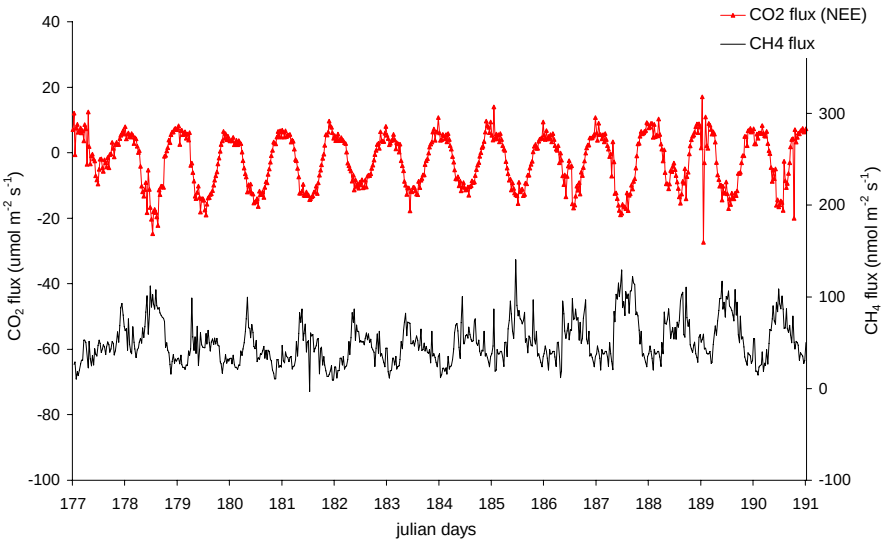

Fig. 8. Graph of CH_4 flux data series over a two week period in the summer of 2006, combined with CO_2 flux (NEE) data series over the same period.

ACPD
7, 11587–11619, 2007

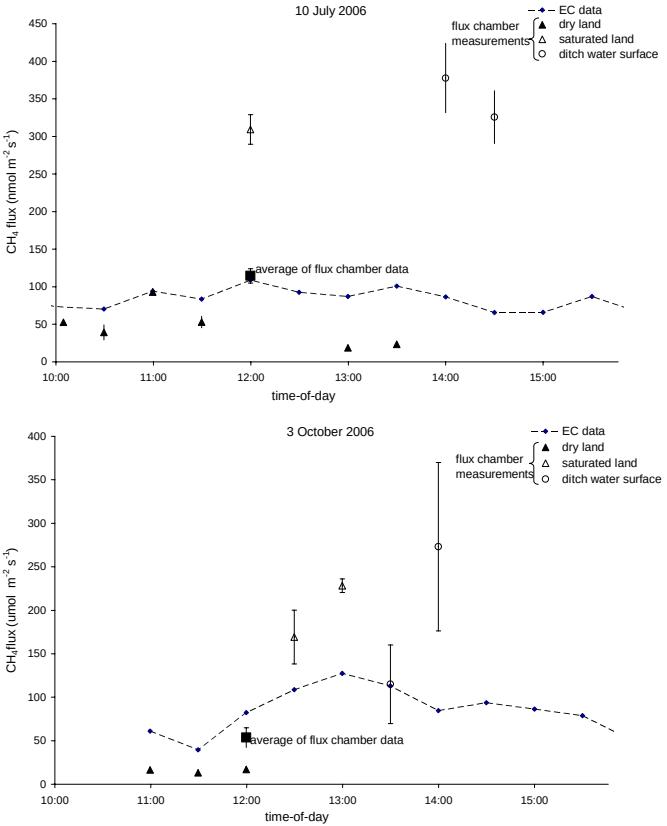

Fig. 9. Hourly CH_4 flux data at 10 July and 3 October the (both 2006) plotted in combination with flux chamber data from various land elements in the footprint of the eddy covariance tower collected at the same day. Additionally, the weighed average of the flux chamber measurements is shown.

ACPD
7, 11587–11619, 2007

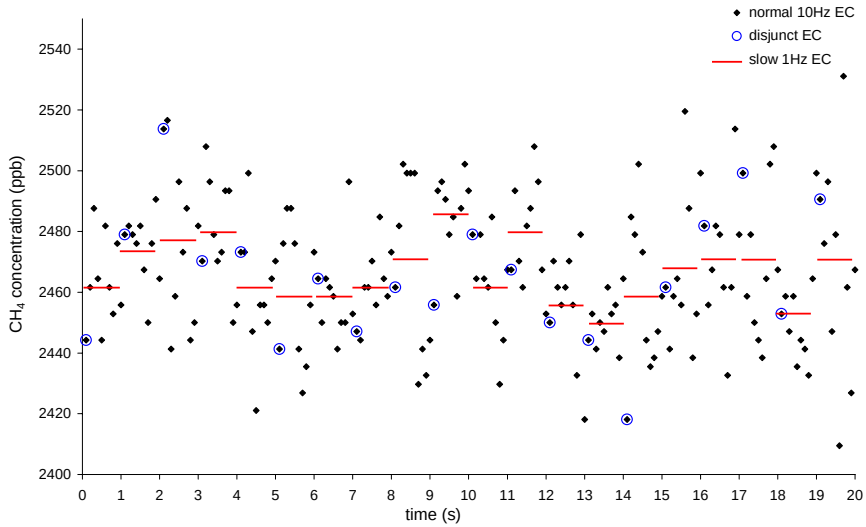

Fig. 10. Example of data sampling for the various measurement types: measured concentrations for normal 10 Hz eddy covariances, disjunct eddy covariance and slow 1 Hz eddy covariance. Disjunct eddy covariance takes every first sample point of a 10 Hz data series and slow eddy covariance takes the average of ten sample points of a 10 Hz data series.

ACPD
7, 11587–11619, 2007

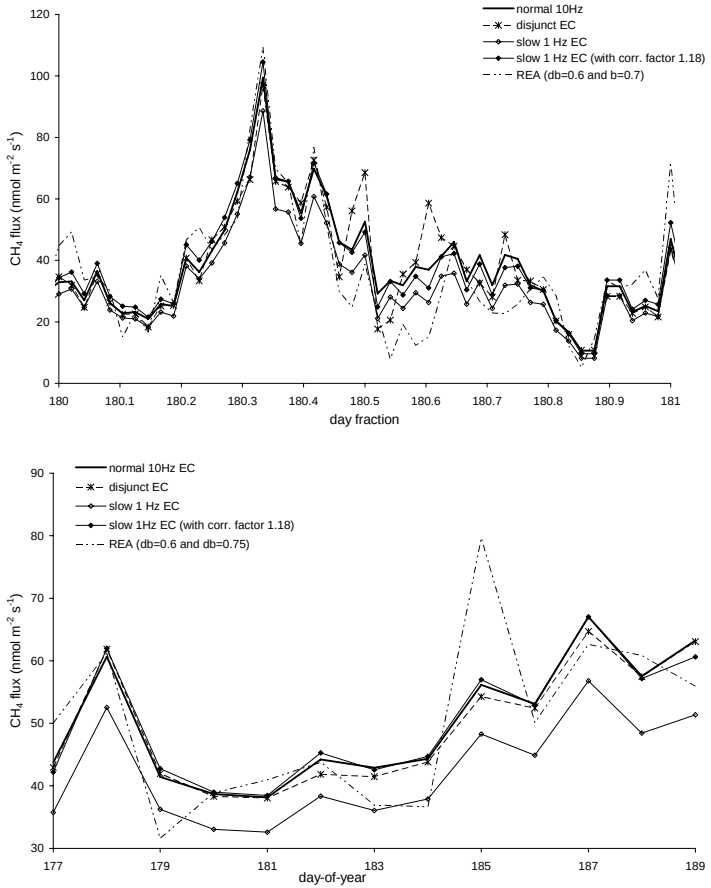

Fig. 11. Time series of CH_4 fluxes: half hourly fluxes over one day (upper graph) and daily CH_4 emissions over a two week period (lower graph) determined by normal 10 Hz eddy covariance, disjunct eddy covariance, slow 1 Hz eddy covariance (with and without correction factor) and REA.

ACPD
7, 11587–11619, 2007